

# Mixed mode crack growth conditions – critical plane approaches.

K.P. Mróz, Z. Mróz and K. Doliński

Institute of Fundamental Technological, Polish Academy of Science, Warsaw (Poland)  
kmroz@ippt.gov.pl

**Keywords:** mixed mode crack growth, critical plane, energy conditions, brittle fracture, ductile fracture, SIF, strain energy density, LEFM.

**Abstract.** The crack growth rules are usually specified in terms of the potential energy release or of non local stress or strain criteria. In the present work, the criteria based on the critical plane concept are first discussed and expressed in terms of averaged stress developed in the crack front domain. The transition from tensile to shear fracture is predicted for varying mode mixity ratio.

## Introduction

The mixed mode crack growth conditions have been analysed extensively for both monotonic and fatigue loading cases. The reviews of Qian and Fatemi [1] and recently by Mróz and Mróz [2] provide discussion of different criteria formulations and assessment of their applicability in quantitative prediction of crack growth, including major aspects, namely crack growth direction and rate of growth. The first group of fracture criteria is based on the potential energy release, expressed in terms of stress intensity factors  $K_I$ , ( $I=1,2,3$ ) or the energy release rates  $G_I$  and the related path independent integrals  $J_I$ . In the second group the fracture criteria are expressed in terms of stress or strain at the distance  $r$  from the crack tip, such as maximal tangential stress criterion (MTS), [3], maximal tangential strain, [4] or criterion expressed in terms of tangential stress or strain, [5], for which their limit values specify crack growth. In the third group, the fracture criteria are expressed in terms of the specific elastic energy at the small distance  $r$ , (S-criterion, [6]) or of the specific volumetric and distortional energies (T-criterion, [7] or MK-criterion [2, 8]). The advantages of using the two energies is that the value of one specific energy provides the radius  $r$  and the stress criterion of crack growth, the value of other provides the crack growth orientation. The critical plane approach provides the criterion in terms of normal and shear stresses acting on this plane with a proper strength function expressing the critical state [9, 10]. By averaging the stress or strain over a finite area of the critical plane, the non-local criteria are generated. In fact, most of stress or strain conditions are of non-local character, as the stress or strain state is specified at finite distance  $r$  from the crack tip or the averaged values are specified.

In the present paper the critical plane criteria are discussed with application to both brittle and ductile failure. The crack growth models for both monotonic and fatigue loading can then be formulated with account for critical plastic strain and material ductility.

## Stress state at the crack front

Consider a plane crack of length  $2a$  in a plate under uniform remote biaxial loading  $\sigma_y = \sigma^\infty$ ,  $\sigma_x = k\sigma^\infty$ , Fig. 1.

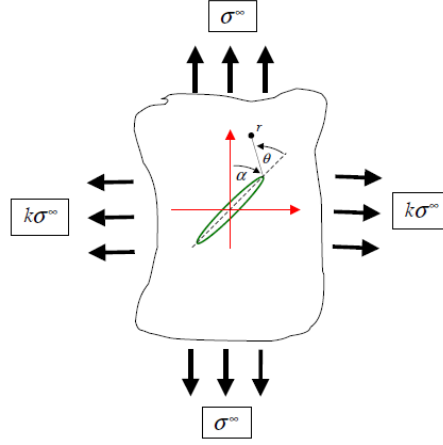


Figure 1. Two dimensional loading conditions.

The asymptotic elastic stress state at the crack front is represented by the sum of singular stress terms. In the local polar coordinate stress system we have

$$\begin{aligned}\sigma_{rr} &\cong \frac{K_I}{\sqrt{2\pi r}} \bar{A}_1 + \frac{K_{II}}{\sqrt{2\pi r}} \bar{A}_2, \\ \sigma_{\theta\theta} &\cong \frac{K_I}{\sqrt{2\pi r}} \bar{B}_1 + \frac{K_{II}}{\sqrt{2\pi r}} \bar{B}_2, \\ \sigma_{r\theta} &\cong \frac{K_I}{\sqrt{2\pi r}} \bar{C}_1 + \frac{K_{II}}{\sqrt{2\pi r}} \bar{C}_2,\end{aligned}\quad (1)$$

where

$$\begin{aligned}\bar{A}_1 &= \frac{5}{4} \cos \frac{\theta}{2} - \frac{1}{4} \cos \frac{3\theta}{2} = \cos \frac{\theta}{2} \left( 1 + \sin^2 \frac{\theta}{2} \right), & \bar{A}_2 &= -\frac{5}{4} \sin \frac{\theta}{2} + \frac{3}{4} \sin \frac{3\theta}{2} = \frac{3}{2} \sin \theta - 2 \tan \frac{\theta}{2}, \\ \bar{B}_1 &= \frac{3}{4} \cos \frac{\theta}{2} + \frac{1}{4} \cos \frac{3\theta}{2} = \cos^3 \frac{\theta}{2}, & \bar{B}_2 &= -\frac{3}{4} \sin \frac{\theta}{2} - \frac{3}{4} \sin \frac{3\theta}{2} = -\frac{3}{2} \cos \frac{\theta}{2} \sin \theta, \\ \bar{C}_1 &= \frac{1}{4} \sin \frac{\theta}{2} + \frac{1}{4} \sin \frac{3\theta}{2} = \frac{1}{2} \cos \frac{\theta}{2} \sin \theta, & \bar{C}_2 &= \frac{1}{4} \cos \frac{\theta}{2} + \frac{3}{4} \cos \frac{3\theta}{2} = \frac{3}{2} \cos \frac{\theta}{2} \cos \theta - \frac{1}{2},\end{aligned}\quad (2)$$

where the angles  $\alpha$  and  $\theta$  are shown in Fig. 1. Under increasing boundary loading the crack growth may occur either in its plane,  $\theta_{pr} = 0$ , or along the direction  $\theta_{pr} \neq 0$  inclined to the crack plane. For the crack inclined at  $\alpha = \pi/2$  to the y-axis the tensile mode I loading occurs and for  $\alpha = \pi/4$ ,  $k = -1$  the shear mode II of loading acts.

The stress intensity factors associated with the singular stress terms are

$$K_I = \sigma^\infty \sqrt{\pi a} (\sin^2 \alpha + k \cos^2 \alpha), \quad K_{II} = \sigma^\infty \sqrt{\pi a} (1 - k) \sin \alpha \cos \alpha \quad (3)$$

and the energy release rates are

$$G_I = K_I^2 / E^*, \quad G_{II} = K_{II}^2 / E^* \quad (4)$$

where  $E^* = E$  for the case of plane stress and  $E^* = E/(1 - \nu^2)$  for the case of plane strain. Denoting the mode mixity by  $m_c$ , we can write

$$m_c = \frac{K_{II}}{K_I} = \sqrt{\frac{G_{II}}{G_I}} = \tan \psi = (1 - k) \frac{\tan \alpha}{\tan^2 \alpha + k} \quad (5)$$

and  $m_c = 0$  when  $\alpha = \pi/2$  or  $\alpha = 0$ ,  $k > 0$ , and  $m_c = \infty$  when  $\alpha = \pi/4$ ,  $k > -1$ .

For the crack growing in its plane the critical state condition is usually specified as follows

$$F_C = R_C(K_I, K_{II}) - 1 = \begin{cases} \left(\frac{K_I}{K_{IC}}\right)^2 + \left(\frac{K_{II}}{K_{IIC}}\right)^2 - 1 \leq 0, & \text{for } K_I > 0, \\ \frac{|K_{II}|}{K_{IIC}} - 1 \leq 0, & \text{for } K_I < 0, \end{cases} \quad (6)$$

where  $K_{IC}$  and  $K_{IIC}$  are the limit values in modes I and II. However, the critical hoop stress condition requires only one parameter  $K_{IC}$  and then  $K_{IIC}$  is predicted by the assumed criterion.

### Critical plane model for crack growth.

There have been numerous formulations of the critical planes models aimed to predict crack growth under monotonic and fatigue loading. Here, we follow the non-local formulation of Seweryn and Mróz [9,10]. Consider a physical plane in the material element specified by a unit normal vector  $\mathbf{n}$ . The plane traction vector and its components then are

$$\mathbf{T} = \boldsymbol{\sigma}\mathbf{n}, \quad \boldsymbol{\sigma}_n = (\mathbf{n} \cdot \boldsymbol{\sigma}\mathbf{n})\mathbf{n}, \quad \boldsymbol{\tau}_n = (\mathbf{I} - \mathbf{n} \otimes \mathbf{n})\boldsymbol{\sigma}\mathbf{n} \quad (7)$$

Where  $\mathbf{I}$  denotes the unit tensor,  $\otimes$  denotes the dyadic product and dot denotes the scalar product. Similarly, the strain components are

$$\boldsymbol{\Gamma} = \boldsymbol{\varepsilon}\mathbf{n}, \quad \boldsymbol{\varepsilon}_n = (\mathbf{n} \cdot \boldsymbol{\varepsilon}\mathbf{n})\mathbf{n}, \quad \boldsymbol{\gamma}_n = (\mathbf{I} - \mathbf{n} \otimes \mathbf{n})\boldsymbol{\varepsilon}\mathbf{n} \quad (8)$$

In the case of brittle fracture it is assumed that crack initiation and growth depend on the surface traction components and the resulting crack opening and shear displacement provide the damage strains of the material element. The stress components  $\boldsymbol{\sigma}_n, \boldsymbol{\tau}_n$  are now used to express the crack growth condition. Assume the elliptical form for  $\boldsymbol{\sigma}_n \geq 0$  and the Coulomb condition for  $\boldsymbol{\sigma}_n \leq 0$ , so we have

$$F_C = R_C(K_I, K_{II}) - 1 = \max_n \begin{cases} \sqrt{\left(\frac{\boldsymbol{\sigma}_n}{\boldsymbol{\sigma}_C}\right)^2 + \left(\frac{\boldsymbol{\tau}_n}{\boldsymbol{\tau}_C}\right)^2} - 1 \leq 0, & \text{for } \boldsymbol{\sigma}_n \geq 0, \\ \frac{|\boldsymbol{\tau}_n| + \boldsymbol{\sigma}_n \tan \varphi}{\boldsymbol{\tau}_C} - 1 \leq 0, & \text{for } \boldsymbol{\sigma}_n < 0, \end{cases} \quad (9)$$

Where  $\boldsymbol{\sigma}_C, \boldsymbol{\tau}_C$  denote the failure stresses in tension and shear and  $\varphi$  denotes the friction angle at the compressed crack interface. For a singular stress state the non-local stress failure condition is applied by averaging the normal and shear stress components on a plane element area  $r_0 \times r_0$ , thus

$$\bar{\boldsymbol{\sigma}}_n = \frac{1}{r_0^2} \int_0^{r_0} \int_0^{r_0} \boldsymbol{\sigma}_n d\xi_1 d\xi_2, \quad \bar{\boldsymbol{\tau}}_n = \frac{1}{r_0^2} \int_0^{r_0} \int_0^{r_0} \boldsymbol{\tau}_n d\xi_1 d\xi_2 \quad (10)$$

and applying the crack growth condition in the form

$$F_C = \bar{R} - 1 = \max_n \left[ \bar{R}(\bar{\boldsymbol{\sigma}}_n, \bar{\boldsymbol{\tau}}_n) - 1 \leq 0 \right] \quad (11)$$

The size parameter  $r_0$  represents the size of damage zone and can be specified from the formula

$$r_0 = \frac{1}{2\pi} \left[ M_C \left( \frac{K_{IC}}{\boldsymbol{\sigma}_C} \right)^2 + (1 - M_C) \left( \frac{K_{IIC}}{\boldsymbol{\tau}_C} \right)^2 \right], \quad M_C = \cos \psi = \frac{K_I}{\sqrt{K_I^2 + K_{II}^2}} = \frac{1}{\sqrt{1 + m_C^2}} \quad (12)$$

assuming transition to the Griffith conditions for tension and shear modes. Let us note that the stress condition (9) parallels the energy condition (7) and requires two stress parameters. The application of condition (9) to predict crack growth in fatigue loading was presented in [10].

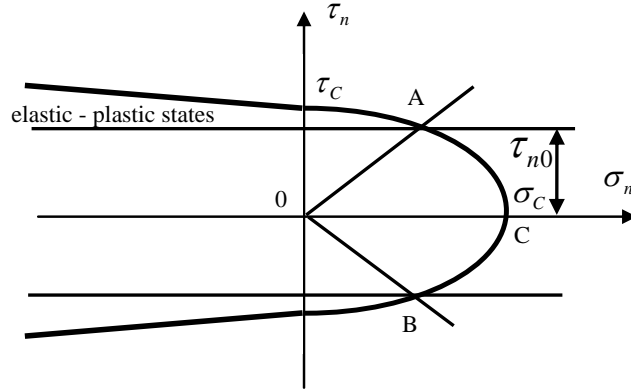


Figure 2. The limit state locus for brittle-ductile fracture.

The application to brittle and ductile failure conditions requires to account for plastic deformation and material ductility. Referring the stress state to the maximal shear plane, the value of yield stress  $\tau_y$  can be introduced, Fig. 2. This value specifies the limit stress state ABC of brittle response and the elastic – plastic states bounded by the limit surface. The transition from brittle to ductile response at A and B now is specified by the mode mixity ratio  $\sigma_n / \tau_{n0}$ . To avoid elastic – plastic analysis, a simplified approach is proposed by applying the elastic singular stress distribution and the strength function  $\bar{R}$  in the form

$$\bar{R} = \max_{\theta} \left( \left( \frac{\sigma_{\theta\theta}(r_0, \theta)}{\sigma_c} \right)^p + \left( \frac{\tau_{r\theta}(r_0, \theta)}{\tau_c} \right)^p \right)^{1/p} \quad \text{for} \quad p = 2, 3, 4, \dots \quad (13)$$

As discussed by Chao and Liu [11], the fracture criterion is based on the competition of tensile fracture associated with the limit strength  $\sigma_c$  and shear fracture associated with the limit strength,  $\tau_c$ . The transition from tensile to shear mode is observed for varying mode mixity parameter  $M_c$ , Fig. 3. The results are compared to experimental data from Hallback and Nilsson [12] and Maccagno and Knott [13] for two different material: PMMA and aluminum 7075-T6, cf. Table 1.

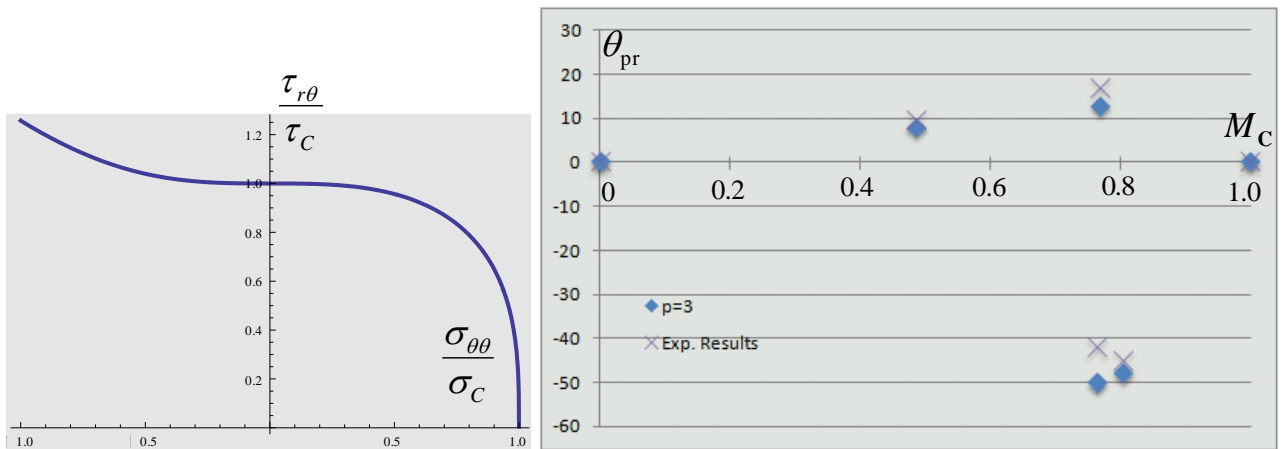


Figure 3. (a) The sketch of  $\bar{R}$  function for  $p=3$ . (b) Comparison of the angle of crack propagation for function  $\bar{R}$  and  $p=3$ , based on the experimental data [12], AC1-specimen.

## Predicted of crack growth orientation - results.

The model predictions for varying values of exponent  $p$  are presented in Table 2 and compared with the aluminium data. Figures 3a,b present the failure locus and the evolution of crack orientation varying with the mode mixity ratio. Figures 4-9 illustrate the evolution of the strength function  $\bar{R}$  for varying critical plane orientation and specification of the crack propagation direction.

material	Shear strength $\tau_c$ [MPa]	Tensile strength $\sigma_c$ [MPa]
PMMA	80	63
Aluminium 7075-T6	330	570

Table 1. Assumed material data.

$K_I$	$K_{II}$	$M_C$	$\theta_{pr}$ for $p=2$	$\theta_{pr}$ for $p=3$	$\theta_{pr}$ for $p=4$	Exp. Data [w12] $\theta_{pr}$
0	48,07	0	0	0	0	0
20,5	37,38	0,48	-0,08	7,8	8,7	9,5
34,6	28,75	0,77	-0,19	12,72	-50,1	17
39,8	33,4	0,768	-0,19	-50,21	-50,39	-42
40,5	29,9	0,8	-0,19	-48	18,3	-45
31,2	0	1	0	0	0	0

Table 2. Comparison of the angle of crack propagation for function  $\bar{R}$  and  $p=2,3,4$ , based on the experimental data [12], AC1-specimen.

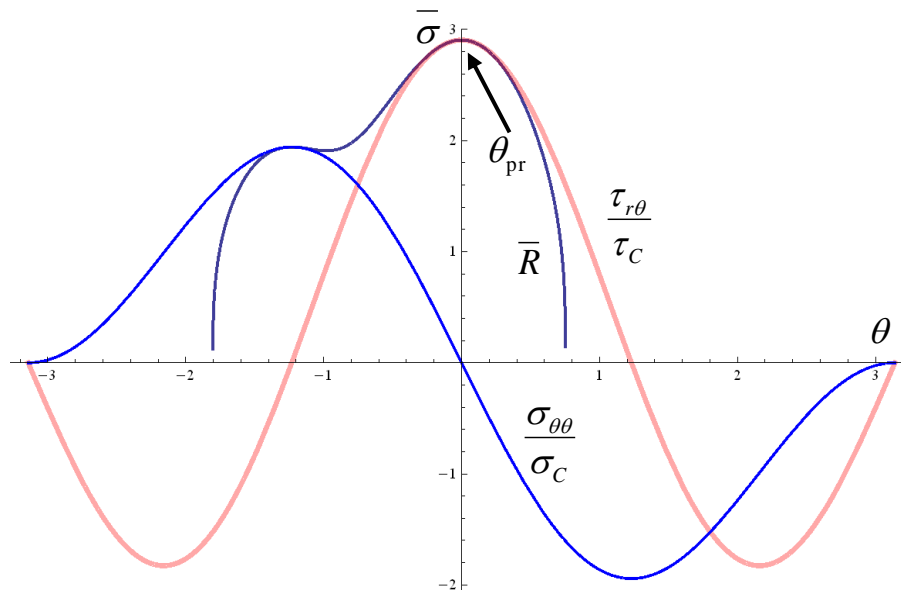


Figure 4. Results according to [11,12] for  $K_I=0, K_{II}=48.07$  and  $M_C=0$ . Shear fracture (aluminium).

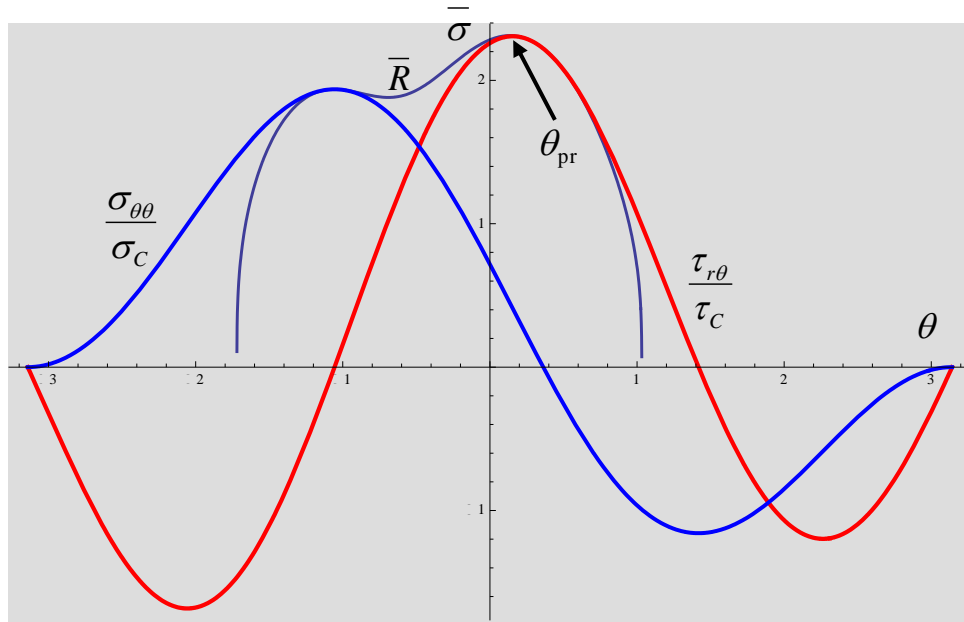


Figure 5. Results according to [11,12] for  $K_I = 20.5, K_{II} = 37.38$  and  $M_C = 0.48$ . Shear fracture (aluminium).

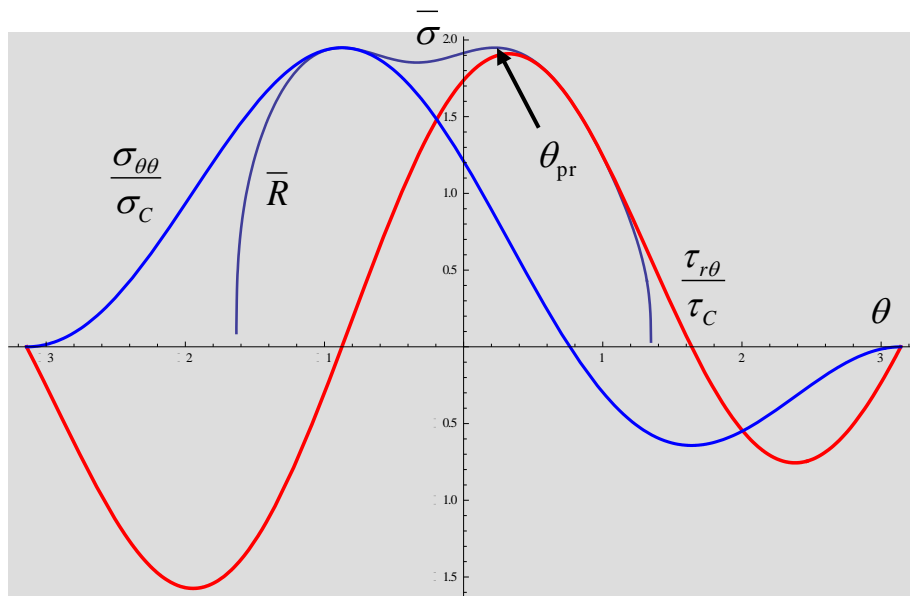


Figure 6. Results according to [11,12] for  $K_I = 34.6, K_{II} = 28.75$  and  $M_C = 0.77$ . Shear fracture (aluminium).

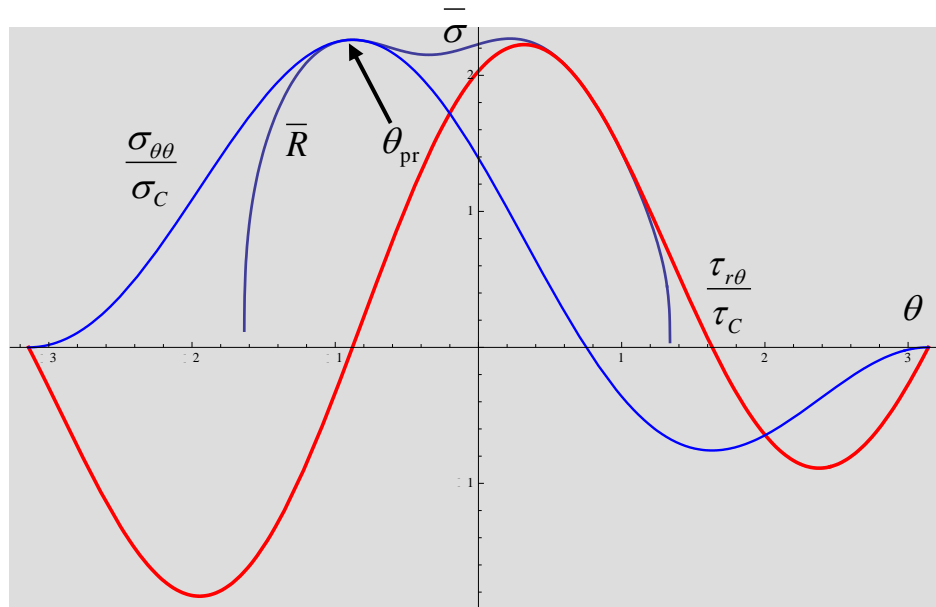


Figure 7. Results according to [11,12] for  $K_I = 39.8, K_{II} = 33.4$  and  $M_C = 0.768$ . Tensile fracture (aluminium).

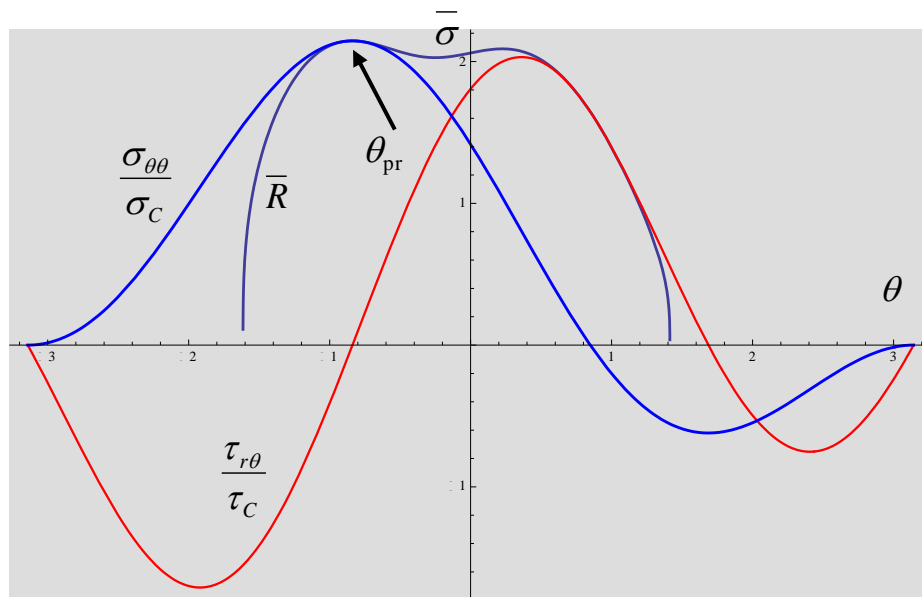


Figure 8. Results according to [11,12] for  $K_I = 40.5, K_{II} = 29.9$  and  $M_C = 0.8$ . Tensile fracture (aluminium).

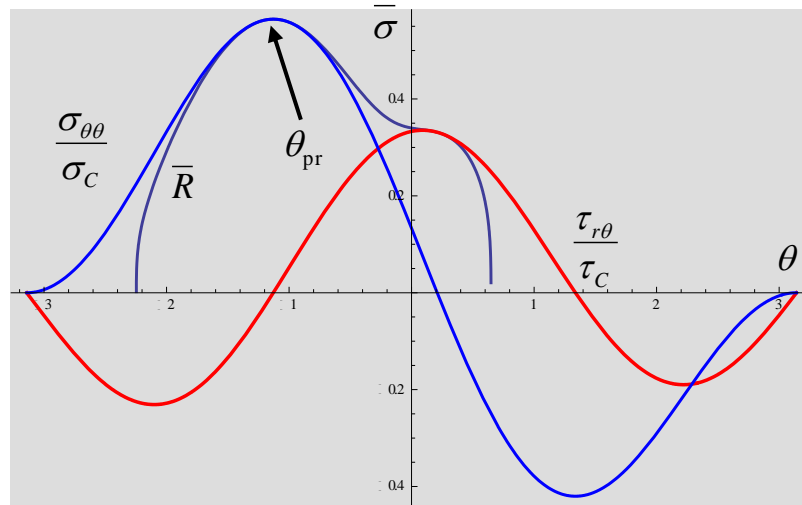


Figure 9. Results according to [11,13] for  $K_I = 0.42, K_{II} = 1.336$  and  $M_C = 0.30$ . Tensile fracture (PMMA).

## Conclusion

The present paper provides the description of fracture mode evolution for varying mode mixity parameter. The critical plane condition was used and the failure locus was specified in the stress plane  $\frac{\sigma_n}{\sigma_C}, \frac{\tau_n}{\tau_C}$  where  $\sigma_C, \tau_C$  are the limit stress values. The material ductility effect can be simulated by assuming  $\sigma_C = \sigma_C(\varepsilon_{ft}), \tau_C = \tau_C(\varepsilon_{fs})$ , where  $\varepsilon_{ft}$  and  $\varepsilon_{fs}$  are limit plastic strains in tension and shear.

## References

- [1] J. Qian and A. Fatemi: Eng. Fract. Mech. Vol.55 (1996), p.969-990.
- [2] K. P. Mróz and Z. Mróz: Eng. Fract. Mech. 77 (2010) , p.1781–1807.
- [3] F. Erdogan and G.C. Sih: J Basic Engng Vol. 85 (1963), p. 519–527.
- [4] A.C. Chambers , T.H. Hyde and J.J. Webster: Engng Fract. Mech Vol.39 (1991), p.603–619.
- [5] X. Wu and X. Li: Engng Fract. Mech. Vol. 34 (1989), p.55–64.
- [6] G.C. Sih: Engng Fract Mech Vol. 5 (1973), p.365–377.
- [7] P.S. Theocaris and N.P. Andrianopoulos: Engng Fract Mech Vol. 16 (1982), p.425–432.
- [8] K. P. Mróz and K. Doliński: Z. Angew. Math. Mech. Vol. 90 (2010), p.721 –744.
- [9] A. Seweryn and Z. Mróz: Engng Fract Mech. Vol. 51 (1995), p.955–973.
- [10] A. Seweryn and Z. Mróz: Int J Solids Struct. Vol. 35 (1998), p.1589–616.
- [11] Y.J. Chao and S. Liu: International Journal of Fracture Vol. 87 (1997), p.201-223.
- [12] N. Hallback and F. Nilson: Journal of the Mechanics and Physics of Solids Vol. 42 (1994), p. 1345-1374.
- [13] T.M. Maccagno and J.F. Knott: Engineering Fracture Mechanics Vol. 34 (1989), p. 65-86.